Journal of Biomedical Optics

BiomedicalOptics.SPIEDigitalLibrary.org

Measurement of refractive index of hemoglobin in the visible/NIR spectral range

Ekaterina N. Lazareva
Valery V. Tuchin

SPIE.

Ekaterina N. Lazareva, Valery V. Tuchin, "Measurement of refractive index of hemoglobin in the visible/NIR spectral range," *J. Biomed. Opt.* **23**(3), 035004 (2018), doi: 10.1117/1.JBO.23.3.035004.

Measurement of refractive index of hemoglobin in the visible/NIR spectral range

Ekaterina N. Lazareva[a,b,*] **and Valery V. Tuchin**[a,c,d]
[a]Saratov State University (National Research University), Research Educational Institute of Optics and Biophotonics, Saratov, Russia
[b]Immanuel Kant Baltic Federal University, Center for Functionalized Magnetic Materials (FunMagMa), Kaliningrad, Russia
[c]Tomsk State University (National Research University), Interdisciplinary Laboratory of Biophotonics, Tomsk, Russia
[d]Institute of Precision Mechanics and Control RAS, Laboratory of Laser Diagnostics of Technical and Living Systems, Saratov, Russia

Abstract. This study is focused on the measurements of the refractive index of hemoglobin solutions in the visible/near-infrared (NIR) spectral range at room temperature for characteristic laser wavelengths: 480, 486, 546, 589, 644, 656, 680, 930, 1100, 1300, and 1550 nm. Measurements were performed using the multi-wavelength Abbe refractometer. Aqua hemoglobin solutions of different concentrations obtained from human whole blood were investigated. The specific increment of refractive index on hemoglobin concentration and the Sellmeier coefficients were calculated. [DOI: 10.1117/1.JBO.23.3.035004]

Keywords: hemoglobin; refractive index; dispersion; Sellmeier coefficients; specific refraction increment.

Paper 170750R received Nov. 21, 2017; accepted for publication Feb. 20, 2018; published online Mar. 15, 2018.

1 Introduction

The refractive index (RI) of biological tissue is a basic material parameter that characterizes how light interacts with tissue.[1] In many optical studies, a rough estimate of RI of the tissue under study, based on the fact that the main constituent of tissue is salt water-filled cells or more precisely a mixture of salt water and proteins, is often used.[2,3] For many tissues and blood components, the data for RI in a wide spectral range and concentrations are not yet available.[4]

The study of optical properties of hemoglobin is important for the development of diagnostic and laser treatment techniques, where consideration of blood optical properties is critical. Various optical methods widely used for tissue characterization, such as visible and near-infrared (NIR) spectroscopy, optical coherence tomography, and fluorescence spectroscopy, need exact data for RI of tissue, blood, and their components to quantify properly experimental data.[5–11]

At present, the usage of RI as a diagnostic marker is urgent.[5–20] Sometimes, it is a self-sufficient parameter for tissue and blood characterization. Zhernovaya et al. considered the change of RI of hemoglobin and albumin at the interaction with glucose as a possible method for studying the glycation process and determining glycated proteins, which is important for the monitoring of diabetes mellitus.[9] The RI of tissue was used as a marker for cancer, reflecting changes of optical properties in the course of pathology development.[10,11,14–20] An additional motivation for this study is a lot of discrepancies between the RIs reported in the literature by different research groups.

The RI is a complex value consisting of a real part n, which represents the ratio of the speed of light in a vacuum to the speed of light in the material $n = c/v$, and an imaginary part k, which represents light attenuation[21–25]

$$\tilde{n} = n + ik. \tag{1}$$

Because of tissue heterogeneity, n is always known as the effective or average RI.[24,26] According to the classical theory of light dispersion, the components of the complex RI of molecular structures can be written as[21–25]

$$n = 1 + \frac{2\pi q^2 N(\omega_0^2 - \omega^2)}{m(\omega_0^2 - \omega^2)^2 + \gamma^2\omega^2}, \tag{2}$$

$$k = \frac{2\pi q^2 N\gamma\omega}{m(\omega_0^2 - \omega^2)^2 + \gamma^2\omega^2}, \tag{3}$$

where q is the molecular charge, N is the number of molecules per unit volume, m is the molecular mass, ω is the probing light frequency, ω_0 is the central frequency of molecular absorption band, and γ is the attenuation coefficient.[21–25]

Over the last decades, various techniques to determine RI of biological tissues were developed; they include confocal microscopy,[1,6] optical fiber cladding method,[27] minimum deviation angle method,[28,29] optical coherent tomography with multiple modifications,[6,9,30–36] total internal reflection method,[26,37,38] measurement of the intensity profile of diffuse light refracted into the prism around the critical angle,[39] various modifications of nonlinear phase microscopy,[40–42] and quantitative phase imaging techniques.[12,43,44]

Because of the strong hemoglobin absorption, direct measurements of the real part of RI using conventional refractometers (for example, an Abbe refractometer) have proven to be difficult, and data are available at a few wavelengths only. In an early study, for example, Barer measured n for solutions of oxygenated hemoglobin at 589 nm only.[44] He also discussed RI dependence on the hemoglobin concentration and presented the expression

*Address all correspondence to: Ekaterina N. Lazareva, E-mail: Lazarevaen@list.ru

1083-3668/2018/$25.00 © 2018 SPIE

$$n = n_{H_2O} + \alpha C, \tag{4}$$

where n_{H_2O} is the RI of distilled water, C is the concentration of hemoglobin, and α is the specific refraction increment.[44]

Faber et al. measured the RI of solutions of oxygenated and deoxygenated hemoglobin at 800 nm.[45] Friebel and Meinke measured directly the RI of solutions of oxygenated hemoglobin at 633 nm for several concentrations[7,8]

$$n = n_{H_2O}(1 + \beta C). \tag{5}$$

Zhernovaya et al. also used the formula similar to Eq. (4) to describe the linear dependence of the RI of hemoglobin on the concentration

$$n = n_0 + \alpha C, \tag{6}$$

where n_0 is the RI of solvent, C is the hemoglobin concentration in dl/g, and α is the specific refraction increment.[4,46]

Jin et al. measured RI of hemoglobin solution at 633 and 532 nm using a total internal reflection technique.[37] Park et al. measured the dispersion of Hb solutions, prepared from Hb protein powder, at 440, 546, 560, 580, 600, 655, and 700 nm using spectroscopic phase microscopy.[41] Deng et al. showed that, in the 400 to 750 nm range, hemoglobin solution is characterized by specific forms of dispersion and extinction spectra.[47] Yahya and Saghir measured RIs for multiple temperatures and wavelengths using the Abbemat refractometer.[48] They found linear dependences of RI on hemoglobin concentration and temperature and nonlinear on the wavelength.

Analysis of the dispersion relation in similar studies showed significant differences for oxyhemoglobin and deoxyhemoglobin, related to the difference in the imaginary part of the RI for the 500 to 600 nm region.[4,45–50] There is lack of data for RI of hemoglobin solutions for concentrations close to that in the red blood cells (RBC), especially for the NIR region.

This study is focused on the determination of the RI of hemoglobin in the visible and NIR ranges at room temperature, aiming for further quantification dispersion of hemoglobin solutions. Measurements were carried out using the multiwavelength Abbe refractometer (Atago, Japan). The hemoglobin solutions of different concentrations obtained from human whole blood were investigated. The RI of hemoglobin solutions was measured for the wavelengths: 480, 486, 546, 589, 644, 656, 680, 930, 1100, 1300, and 1550 nm, which are characteristic for different lasers widely used in biomedicine. The specific increment of RI and Sellmeier coefficients for dispersion on hemoglobin concentration were calculated based on the experimental data.

2 Methods and Materials

Hemoglobin obtained from human whole blood was used to prepare hemoglobin specimens. Whole blood was drawn from the human vein. Immediately after collecting blood into a test tube, heparin was added in it. The sample of blood from a healthy person was taken at the State Healthcare Organization "Saratov City Clinical Hospital No. 2 named after V. I. Razumovsky" with the permission of the volunteer. To separate blood into fractions, the centrifugation for 10 min at 2000 rpm and at room temperature was provided. This resulted in separation of blood plasma, leuko-platelet layer, and RBC suspension. To conduct hemolysis and preparation of hemoglobin solutions, RBC suspension was separated and placed in a vial for freezing in a freezer at a temperature of −15°C for 24 h.

Fig. 1 General view of the multiwavelength Abbe refractometer (Atago, Japan): 1, refractometer; 2,–power supply; 3, light source; 4, the eyepiece imager for measurements in the NIR region; 5, interference filter; and 6, sample.

Actual concentration of the basic hemoglobin solution was estimated by the spectral technique and amounted to 260 g/l. In the experiment, we measured the RI of three specimens taken from the same sample. The RI measurements for solutions of different concentrations obtained by diluting the basic solution of hemoglobin in saline solution were also provided.

At measurements, a sample layer on the working surface of the prism had a small thickness of about 20 to 30 μm. The time of the full oxygenation (78.4% to 94.2%) of hemoglobin in such a layer is about 6 to 10 s.[51] Therefore, hemoglobin is fully saturated with oxygen, and the process of oxygenation during measurements is expected to not affect the result.

Measurements were performed using the multiwavelength Abbe refractometer (Atago, Japan) (Fig. 1). The RI was measured for samples of hemoglobin obtained from human whole blood (65, 87, 173, and 260 g/l) on 11 wavelengths from 480 to 1550 nm. The temperature was 23°C.

Multiwavelength refractometer Abbe allows one to measure the RI in the wavelength range of 450 to 1550 nm with an accuracy of ±0.0002. The working principle of the refractometer technique is based on determining the critical angle of the total reflection, where the incident light waves are completely reflected with a 90-deg angle to the normal position. The incident light waves with angles greater than the critical angle will only experience reflection at the interface surface and no refraction will be observed. The total internal reflection method is applicable to measurement of the RI of biological media,

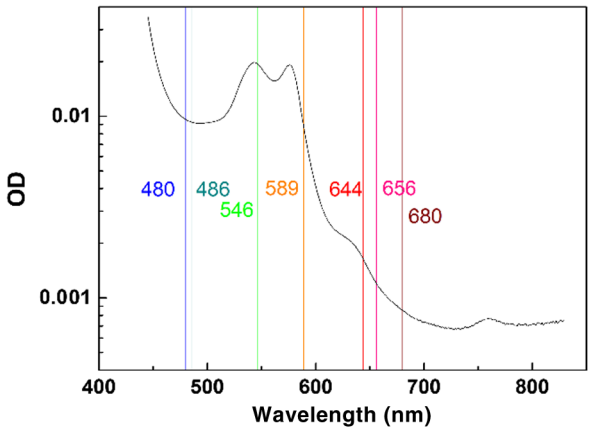

Fig. 2 The optical density spectrum of a solution of hemoglobin 260 g/l. By the vertical lines visible working wavelengths of Atago refractometer are shown.

which are characterized by high light scattering and absorption. The wavelength of the light source is determined by the selection of the particular interferential filter. Available interferential filters allowed for measurements on the wavelengths 480 ± 2, 486 ± 2, 546 ± 2, 589 ± 2, 644 ± 2, and 656 ± 2 nm, 680 ± 5, 930 ± 6, 1100 ± 26, 1300 ± 25, and 1550 ± 25 nm. The calibration of the device by measuring RI of distilled water at a wavelength of 589 nm (the absorption band of sodium) was used at the beginning of each experiment. The average measurement error of the RI was ± 0.0003.

To approximate the dispersion dependence of the RI of the hemoglobin solution, the Sellmeier formula was used

$$n^2(\lambda) = 1 + \frac{A1 * \lambda^2}{\lambda^2 - B1} + \frac{A2 * \lambda^2}{\lambda^2 - B2}, \tag{7}$$

where $A1$, $A2$, $B1$, and $B2$ are empirical constants. Sellmeier's formula gives a good agreement for describing the dispersion dependence of the RI of multicomponent systems near absorption bands of a medium under study.[52] Mathematical calculations were performed in the software package Origin ProLab.

3 Measurement Results

The optical density spectra of a solution of hemoglobin obtained from the whole blood by hemolysis are shown in Fig. 2. The graph shows that the wavelengths available for RI measurements, i.e., 480, 486, 546, 589, 644, and 656 nm, belong to different or the same absorption bands of hemoglobin with quite different absorption abilities. Therefore, we can expect different inclusion of anomalous dispersion in RI wavelength dependence at these wavelengths. Wavelength 546 nm is the closest to the isobestic point 544 nm, where the absorption of hemoglobin does not depend on the degree of oxygenation.[53]

Table 1 presents data for Atago refractometer measurements of RI for four different concentrations of hemoglobin, i.e., 65, 87, 173, and 260 g/l at room temperature, 23°C.

It is well known that the RI of proteins is nonlinearly dependent on the wavelength.[4,45–50,54] Figure 3 shows the dispersion curves for hemoglobin solutions in the visible/NIR spectral range. The symbols are experimental data from Table 1, and the lines correspond to the fit of these data to the Sellmeier formula, Eq. (7). Table 2 presents data for the decomposition of the Sellmeier formula.

As it follows from Table 2, for all wavelengths and hemoglobin concentrations, measured RIs are well fit to the Sellmeier formula with correlation coefficient, R^2, equal or better than 0.993. Specifically, there is a linear relationship between the RI and hemoglobin concentration. The RI of the hemoglobin samples is also temperature-dependent, although the temperature effect on the RI is small when compared with the hemoglobin concentration effect. Figure 4 shows the dependence of the RI of human hemoglobin solution on hemoglobin concentration for the room temperature of 23°C. These data can be used to predict the hemoglobin concentration of the blood sample based on the knowledge of the RI and using the refraction increment provided. This dependence can be described by Eqs. (4) and (5).

Table 1 RI measured for four different concentrations of hemoglobin at room temperature 23°C. SD is shown in brackets.

λ (nm)	0 g/l	65 g/l	87 g/l	173 g/l	260 g/l
480	1.3371 (0.0003)	1.3476 (0.0003)	1.3571 (0.0003)	1.3728 (0.0003)	1.3879 (0.0002)
486	1.3371 (0.0002)	1.3478 (0.0002)	1.3563 (0.0002)	1.3721 (0.0002)	1.3871 (0.0004)
546	1.3342 (0.0002)	1.3448 (0.0002)	1.3533 (0.0002)	1.3681 (0.0007)	1.3836 (0.0002)
589	1.3329 (0.0002)	1.3438 (0.0002)	1.3519 (0.0003)	1.3667 (0.0004)	1.3821 (0.0004)
644	1.3313 (0.0002)	1.3419 (0.0002)	1.3497 (0.0002)	1.3640 (0.0003)	1.3801 (0.0003)
656	1.3308 (0.0002)	1.3414 (0.0002)	1.3493 (0.0002)	1.3647 (0.0003)	1.3792 (0.0009)
680	1.3301 (0.0002)	1.3403 (0.0003)	1.3482 (0.0003)	1.3633 (0.0003)	1.3771 (0.0002)
930	1.3259 (0.0002)	1.3360 (0.0002)	1.3440 (0.0002)	1.3572 (0.0003)	1.3735 (0.0007)
1100	1.3222 (0.0002)	1.3329 (0.0002)	1.3411 (0.0002)	1.3542 (0.0002)	1.3690 (0.0006)
1300	1.3174 (0.0002)	1.3280 (0.0005)	1.3364 (0.0002)	1.3503 (0.0002)	1.3642 (0.0004)
1550	1.3140 (0.0002)	1.3244 (0.0004)	1.3314 (0.0003)	1.3458 (0.0002)	1.3598 (0.0004)

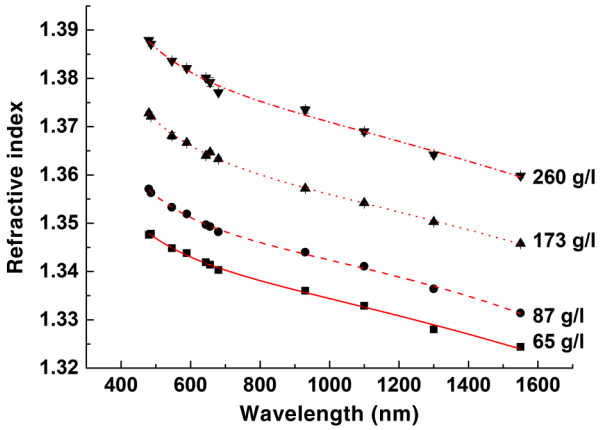

Fig. 3 The dispersion curves for hemoglobin solutions: the symbols are experimental data from Table 1 and the lines correspond to the fit of these data to the Sellmeier formula, Eq. (7).

Table 2 Coefficients of Sellmeier formula for hemoglobin solutions of different concentrations.

Hb (g/l)	$A1$	A_2	$B1$ (1/nm^2)	$B2$, 10^7 (1/nm^2)	R^2
65	0.79099	685.08237	8366.45239	4024.35	0.995
87	0.80835	450.24119	9983.69749	2842.83	0.999
173	0.84507	402.89873	11065.32117	2540.72	0.998
260	0.88871	190.95319	10187.17167	1039.98	0.993

Table 3 presents data for the RI of distilled water and the specific increment of RI for hemoglobin solutions obtained by hemolysis. Approximation of the dependence of the specific increment of the RI on the wavelength was performed using the software package OriginProLab. The best fit was achieved using

$$y = \frac{Cx}{(D + x)}, \tag{8}$$

where $C = 0.17263 \pm 0.00157$ and $D = -57.8324 \pm 5.56032$. The correlation coefficient was $R^2 = 0.90$.

Table 3 The distilled water RI n_{H_2O} and the specific increment dn/dC of RI for hemoglobin solutions obtained by hemolysis, for the room temperature 23°C. SD is shown in brackets.

λ (nm)	n_{H_2O}	α (ml/g)	β (ml/g)
480	1.3371 (0.0003)	0.199 (0.006)	0.149 (0.005)
486	1.3371 (0.0002)	0.196 (0.005)	0.147 (0.004)
546	1.3342 (0.0001)	0.193 (0.005)	0.144 (0.004)
589	1.3329 (0.0002)	0.192 (0.005)	0.144 (0.003)
644	1.3313 (0.0002)	0.189 (0.004)	0.142 (0.003)
656	1.3308 (0.0002)	0.190 (0.005)	0.143 (0.003)
680	1.3301 (0.0001)	0.185 (0.005)	0.139 (0.004)
930	1.3259 (0.0002)	0.183 (0.004)	0.138 (0.003)
1100	1.3222 (0.0002)	0.183 (0.005)	0.139 (0.004)
1300	1.3174 (0.0002)	0.185 (0.006)	0.140 (0.004)
1550	1.3140 (0.0002)	0.179 (0.004)	0.136 (0.003)

4 Discussion

The results of the measurements revealed that there is a linear relationship between the RI and hemoglobin concentration. Table 4 summarizes data on hemoglobin RI available in the literature. The comparison of received data with the literature is presented.

There is lack of data on the RI measurement of hemoglobin solutions for concentrations close to that in the RBC; specifically, data for the NIR region are practically absent. The RI of hemoglobin solution of 260 g/l, obtained from whole blood at room temperature (23°C) for the wavelength of 480 nm, was found to be equal to 1.3879 ± 0.0002, for 589 nm to 1.3821 ± 0.0004, for 1100 nm to 1.3690 ± 0.0006, and for 1550 nm to 1.3598 ± 0.0002. The concentration increment of RI of hemoglobin was found as 0.199 ± 0.006 ml/g for the wavelength 480 nm, 0.192 ± 0.005 ml/g for the wavelength

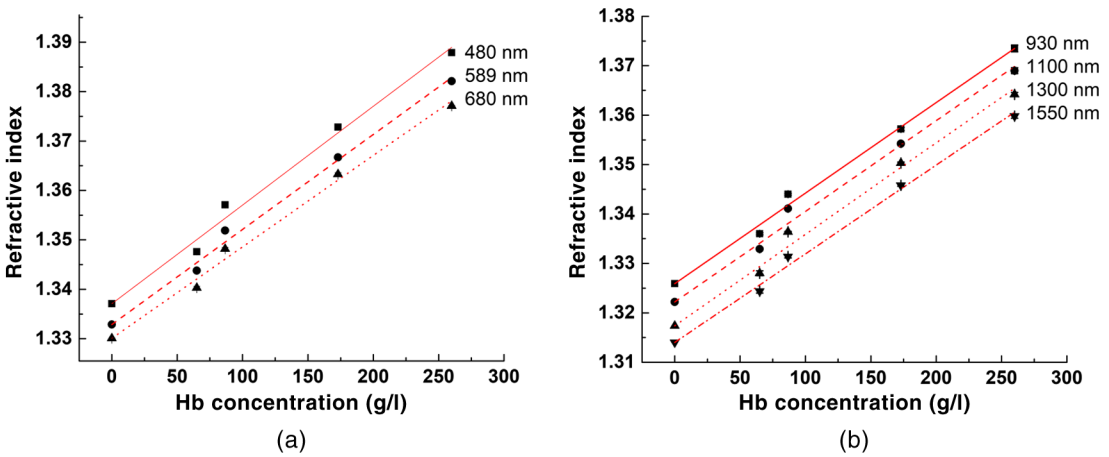

Fig. 4 The dependence of the RI on the concentration of hemoglobin in solution for: (a) visible and (b) NIR ranges (black symbols, experimental data; red lines, approximation of these data).

Table 4 The experimental data for the real part of the RI of the hemoglobin solutions.

λ (nm)	g/l	N	Notes	Ref.
250	46	1.398	Human hemoglobin from fresh RBC suspensions of donors; VIS-NIR-spectrometer	55, 56
	104	1.406		
	165	1.435		
	287	1.470		
300	46	1.373		
	104	1.389		
	165	1.405		
	287	1.441		
400	46	1.354		
	104	1.367		
	165	1.383		
	287	1.409		
400	20	1.35223	Bovine hemoglobin (dry); Hb; pH 7.4; room temperature; continuous RI dispersion (CRID)	47
	40	1.35495		
	60	1.35806		
	80	1.36078		
	120	1.36369		
	140	1.36600		
	280	1.37010		
	320	1.38621		
400	20	1.35107	Bovine hemoglobin (dry); HbO_2; pH 7.4; room temperature; CRID	
	40	1.35417		
	60	1.35767		
	80	1.36039		
	120	1.36369		
	140	1.36602		
	280	1.36951		
	320	1.38660		
400	320	1.3822	Bovine hemoglobin (lyophilized powder); 0.5% HbO_2; $T = 20°C$; fiber spectrometer	26
400	320	1.3775	Bovine hemoglobin (lyophilized powder); Hb; $T = 20°C$; fber spectrometer	
401	140	1.365	Human hemoglobin (lyophilized powder); Hb; $T = 20°C$; pH 7.4; TIR (total internal reflection)	4, 46
435.8		1.367		
401	140	1.369	Human hemoglobin (lyophilized powder); HbO_2; $T = 20°C$; pH 7.4;TIR	
435.8		1.366		
436	150	1.36481	Human hemoglobin (dry); $T = 20°C$; pH 7.4; Abbemat refractometer	48
438	140	1.374	Bovine hemoglobin (dry); Hb; HbO_2; room temperature; pH 7.4	47
440	50	1.3562	Human hemoglobin (lyophilized powder); spectroscopic phase microscopy	41
	150	1.3780		
	300	1.4187		
450	320	1.3888	Bovine hemoglobin (lyophilized powder); 0.5% HbO_2; $T = 20°C$; fiber spectrometer	22
450	320	1.3933	Bovine hemoglobin (lyophilized powder); Hb; $T = 20°C$; fiber spectrometer	
480	65	1.3476 (0.0003)	Human hemoglobin from whole blood; HbO_2; $T = 23°C$; Multiwavelength Abbe refractometer	[a]
	87	1.3571 (0.0003)		
	173	1.3728 (0.0003)		
	260	1.3879 (0.0002)		
486	65	1.3478 (0.0002)	Human hemoglobin from whole blood; HbO_2; $T = 23°C$; Multiwavelength Abbe refractometer	[a]
	87	1.3563 (0.0002)		
	173	1.3721 (0.0002)		
	260	1.3871 (0.0004)		
486.1	140	1.361	Human hemoglobin (lyophilized powder); Hb; $T = 20°C$; pH 7.4; TIR	4, 46
486.1	140	1.361	Human hemoglobin (lyophilized powder); HbO_2; $T = 20°C$; pH 7.4; TIR	
500	287	1.413	Human hemoglobin from fresh RBC suspensions of donors; VIS-NIR-spectrometer	55, 56
	165	1.383		
	104	1.363		
	46	1.348		
500	20	1.34583	Bovine hemoglobin (dry); Hb; pH 7.4; room temperature; CRID	47
	40	1.34913		
	60	1.35223		
	80	1.35592		
	120	1.35922		
	140	1.36175		
	280	1.36544		
	320	1.38408		
500	20	1.34505	Bovine hemoglobin (dry); HbO_2; pH 7.4; room temperature; CRID	
	40	1.34854		
	60	1.35262		
	80	1.35573		
	120	1.35845		
	140	1.36214		
	280	1.36544		
	320	1.38505		
513.9	150	1.36053	Human hemoglobin (dry); $T = 20°C$; pH 7.4; Abbemat refractometer	48
532	1.7	1.3400	Human hemoglobin (fresh human blood); $T = 25°C$; TIR	37
	2.5	1.3431		
	4	1.3485		
	7	1.3604		
	12.97	1.3871		

Table 4 (*Continued*).

λ (nm)	g/l	N	Notes	Ref.
546	65	1.3448 (0.0002)	Human hemoglobin from whole blood; HbO_2; $T = 23°C$; Multiwavelength Abbe refractometer	[a]
	87	1.3533 (0.0002)		
	173	1.3681 (0.0007)		
	260	1.3836 (0.0002)		
546	50	1.3472	Human hemoglobin (lyophilized powder); spectroscopic phase microscopy	41
	150	1.3700		
	300	1.4051		
546.1	140	1.357	Human hemoglobin (lyophilized powder); Hb; $T = 20°C$; pH 7.4; TIR	4, 46
546.1	140	1.357	Human hemoglobin (lyophilized powder); HbO_2; $T = 20°C$; pH 7.4; TIR	
550	320	1.3724	Bovine hemoglobin (lyophilized powder); 0.5% HbO_2; $T = 20°C$; fiber spectrometer	26
550	320	1.3738	Bovine hemoglobin (lyophilized powder); Hb; $T = 20°C$; fiber spectrometer	
560	50	1.3466	Human hemoglobin (lyophilized powder); spectroscopic phase microscopy	41
	150	1.3687		
	300	1.4033		
580	50	1.3451	Human hemoglobin (lyophilized powder); spectroscopic phase microscopy	41
	150	1.3668		
	300	1.4025		
587.6	140	1.356	Human hemoglobin (lyophilized powder); Hb; $T = 20°C$; pH 7.4; TIR	4, 46
587.6	140	1.357	Human hemoglobin (lyophilized powder); HbO_2; $T = 20°C$; pH 7.4; TIR	
589	65	1.3438 (0.0002)	Human hemoglobin from whole blood; HbO_2; $T = 23°C$; multiwavelength Abbe refractometer	[a]
	87	1.3519 (0.0003)		
	173	1.3667 (0.0004)		
	260	1.3821 (0.0004)		
589	46	1.343	Human hemoglobin from fresh RBC suspensions of donors; VIS-NIR-spectrometer	55, 56
	104	1.357		
	165	1.375		
	287	1.406		
589.2	150	1.35724	Human hemoglobin (dry); $T = 20°C$; pH 7.4; Abbemat refractometer	48
589.3	140	1.356	Human hemoglobin (lyophilized powder); Hb; $T = 20°C$; pH 7.4;TIR	4, 46
589.3	140	1.357	Human hemoglobin (lyophilized powder); HbO_2; $T = 20°C$; pH 7.4;TIR	
600	50	1.3443	Human hemoglobin (lyophilized powder); spectroscopic phase microscopy	41
	150	1.3666		
	300	1.4014		

Table 4 (*Continued*).

λ (nm)	g/l	N	Notes	Ref.
600	20	1.34233	Bovine hemoglobin (dry); Hb; pH 7.4; room temperature; CRID	47
	40	1.34485		
	60	1.34874		
	80	1.34835		
	120	1.3520		
	140	1.35495		
	280	1.36155		
	320	1.38233		
600	20	1.34136	Bovine hemoglobin (dry); HbO_2; pH 7.4; room temperature; CRID	
	40	1.34447		
	60	1.34874		
	80	1.35068		
	120	1.35456		
	140	1.35767		
	280	1.36155		
	320	1.38058		
600	320	1.3684	Bovine hemoglobin (lyophilized powder); 0.5% HbO_2; $T = 20°C$; fiber spectrometer	26
600	320	1.3702	Bovine hemoglobin (lyophilized powder); Hb; $T = 20°C$; fiber spectrometer	
632	1.7	1.3626	Human hemoglobin (fresh human blood); $T = 25°C$; TIR	37
	2.5	1.3360		
	4	1.3425		
	7	1.3538		
	12.97	1.3800		
632.8 656.3	140	1.354 1.354	Human hemoglobin (lyophilized powder); Hb; $T = 20°C$; pH 7.4; TIR	4, 46
632.8 656.3	140	1.355 1.354	Human hemoglobin (lyophilized powder); HbO_2; $T = 20°C$; pH 7.4; TIR	
633.2 657.2	150	1.35601 1.35587	Human hemoglobin (dry); $T = 20°C$; pH 7.4; Abbemat refractometer	48
633	104	1.3600	Human hemoglobin (dry); $T = 20°C$; pH 7.4; Abbemat refractometer	56
	165	1.3750		
644	65	1.3419 (0.0002)	Human hemoglobin from whole blood; HbO_2; $T = 23°C$; multiwavelength Abbe refractometer	[a]
	87	1.3497 (0.0002)		
	173	1.3640 (0.0003)		
	260	1.3801 (0.0003)		
650	320	1.3652	Bovine hemoglobin (lyophilized powder); 0.5% HbO_2; $T = 20°C$; fiber spectrometer	26
650	320	1.3668	Bovine hemoglobin (lyophilized powder); Hb; $T = 20°C$; fiber spectrometer	
655	50	1.3408	Human hemoglobin (lyophilized powder); spectroscopic phase microscopy	41
	150	1.3642		
	300	1.3969		

Table 4 (*Continued*).

λ (nm)	g/l	N	Notes	Ref.
656	65	1.3414 (0.0002)	Human hemoglobin from whole blood; HbO_2; $T = 23°C$; multiwavelength Abbe refractometer	[a]
	87	1.3493 (0.0002)		
	173	1.3647 (0.0003)		
	260	1.3792 (0.0009)		
680	65	1.3403 (0.0003)	Human hemoglobin from whole blood; HbO_2; $T = 23°C$; multiwavelength Abbe refractometer	[a]
	87	1.3482 (0.0003)		
	173	1.3633 (0.0003)		
	260	1.3771 (0.0002)		
700	50	1.3405	Human hemoglobin (lyophilized powder); spectroscopic phase microscopy	41
	150	1.3634		
	300	1.3971		
700	20	1.33961	Bovine hemoglobin (dry); Hb; pH 7.4; room temperature; CRID	47
	40	1.34252		
	60	1.34602		
	80	1.34874		
	120	1.35184		
	140	1.35456		
	280	1.35806		
	320	1.37709		
700	20	1.33883	Bovine hemoglobin (dry); HbO_2; pH 7.4; room temperature; CRID	
	40	1.34175		
	60	1.34583		
	80	1.34835		
	120	1.35107		
	140	1.35476		
	280	1.35748		
	320	1.3767		
700	320	1.3612	Bovine hemoglobin (lyophilized powder); 0.5% HbO_2; $T = 20°C$; fiber spectrometer	26
700	320	1.3637	Bovine hemoglobin (lyophilized powder); Hb; $T = 20°C$; fiber spectrometer	
700	46	1.341	Human hemoglobin from fresh RBC suspensions of donors; VIS-NIR-spectrometer	55, 56
	104	1.356		
	165	1.374		
	287	1.404		
706.5	140	1.352	Human hemoglobin (lyophilized powder); Hb; $T = 20°C$; pH 7.4; TIR	4, 46
706.5	140	1.352	Human hemoglobin (lyophilized powder); HbO_2; $T = 20°C$; pH 7.4; TIR	
750	320	1.3589	Bovine hemoglobin (lyophilized powder); 0.5% HbO_2; $T = 20°C$; fiber spectrometer	26
750	320	1.3599	Bovine hemoglobin (lyophilized powder); Hb; $T = 20°C$; Fiber spectrometer	

Table 4 (*Continued*).

λ (nm)	g/l	N	Notes	Ref.
800	46	1.338	Human hemoglobin from fresh RBC suspensions of donors; VIS-NIR-spectrometer	55, 56
	104	1.353		
	165	1.370		
	287	1.400		
900	46	1.338	Human hemoglobin from fresh RBC suspensions of donors; VIS-NIR-spectrometer	55, 56
	104	1.352		
	165	1.369		
	287	1.401		
930	65	1.3360 (0.0002)	Human hemoglobin from whole blood; HbO_2; $T = 23°C$; Multiwavelength Abbe refractometer	[a]
	87	1.3440 (0.0002)		
	173	1.3572 (0.0003)		
	260	1.3735 (0.0007)		
1000	46	1.338	Human hemoglobin from fresh RBC suspensions of donors; VIS-NIR-spectrometer	55, 56
	104	1.353		
	165	1.370		
	287	1.401		
1100	46	1.337	Human hemoglobin from fresh RBC suspensions of donors; VIS-NIR-spectrometer	55, 56
	104	1.352		
	165	1.369		
	287	1.400		
1100	65	1.3329 (0.0002)	Human hemoglobin from whole blood; HbO_2; $T = 23°C$; Multiwavelength Abbe refractometer	[a]
	87	1.3411 (0.0002)		
	173	1.3542 (0.0002)		
	260	1.3690 (0.0006)		
1300	65	1.3280 (0.0005)	Human hemoglobin from whole blood; HbO_2; $T = 23°C$; Multiwavelength Abbe refractometer	[a]
	87	1.3364 (0.0002)		
	173	1.3503 (0.0002)		
	260	1.3642 (0.0004)		
1550	65	1.3244 (0.0004)	Human hemoglobin from whole blood; HbO_2; $T = 23°C$; ultiwavelength Abbe refractometer	[a]
	87	1.3314 (0.0003)		
	173	1.3458 (0.0002)		
	260	1.3598 (0.0004)		

[a]Data from this study.

589 nm, 0.183 ± 0.005 ml/g for the wavelength 930 nm, and 0.179 ± 0.004 ml/g for the wavelength 1550 nm.

Freibel et al. also measured the RI of a hemoglobin solution of 287 g/l obtained from whole blood. According to their measurements using the spectral method and the Fresnel formula, the RI was 1.409 for the wavelength 400 nm, 1.406 for the wavelength 589 nm, 1.404 for the wavelength 700 nm, and 1.400 for the wavelength 1100 nm.[55,56] The same scientific group received at the wavelength 633 nm the RI = 1.3750 for concentration 165 g/l and the RI = 1.3600 for concentration 104 g/l. Jin et al.,[37] Park et al.,[41] Zhernovaya et al.,[46] Yahya et al.,[48] and Deng et al.[47] used a solution obtained from dry hemoglobin for the study of refraction. Zhernovaya et al. measured the RI of oxygenated and deoxygenated hemoglobin of 140 g/l by refractometer Abbe for nine wavelengths at a temperature of 20°C. For example, the values of RI were 1.361 for the wavelength 486 nm, 1.357 for the wavelength 589 nm, and

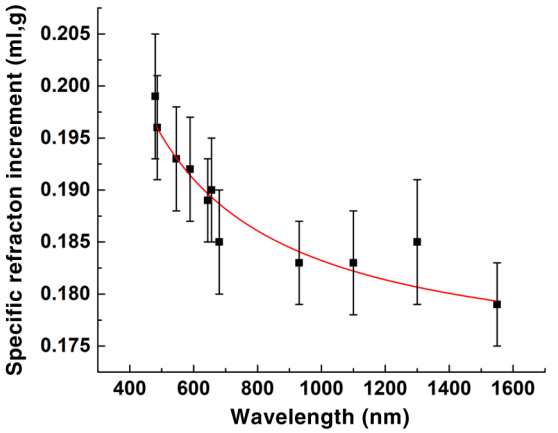

Fig. 5 The dependence of the specific RI increment α of hemoglobin solution on the wavelength (black symbols, estimated data, red lines, approximation of data).

1.352 for the wavelength 706.5 nm.[46] Yahya et al. measured RI of oxygenated human hemoglobin 150 g/l as 1.36481 for the wavelength 436 nm, 1.35724 for the wavelength 589 nm, and 1.35587 for the wavelength 657.2 nm.[48] Deng et al. measured RI of 50% oxyhemoglobin 320 g/l by fiber spectrometer at a temperature of 20°C. RIs were 1.3775 for the wavelength 500 nm, 1.3684 for the wavelength 600 nm, and 1.3612 for the wavelength 700 nm.[47] Jin et al. determined RI of hemoglobin for concentration of 12.97 mmol/l as 1.3871 for the wavelength 532 nm and 1.3800 for the wavelength 632 nm.[37] Park et al. measured the dispersion of Hb solutions, prepared from Hb protein powder, at three different concentrations: 0.05, 0.15, and 0.30 g/ml. For example, the RI for 0.15 g/ml was 1.3687 at wavelength 560 nm.

Zhernovaya et al.,[46] Freibel et al.,[55,56] Yahya et al.,[48] and Park et al.[41] also calculated the specific increment of RI (20°C), which was equal to 0.147, 0.2015, and 0.151 ml/g for the wavelength 589 nm and 0.183 ± 0.003 ml/g for the wavelength range of 440 to 700 nm, respectively. In this study, the RI-specific increment of hemoglobin was found as 0.192 ± 0.005 ml/g for the wavelength 589 nm and temperature at 23°C.

The discrepancy between literature and our data may be caused by the differences in the sample preparation protocols since the human hemoglobin may differ in content of various forms of hemoglobin of donor's blood. The specificities of experimental setups also may play a role.

In Fig. 5, it is seen that the RI-specific increment of a solution of human hemoglobin decreases with the wavelength. This could be explained by the dispersion theory of multicomponent materials and caused by strong absorption bands of hemoglobin and water in UV, hemoglobin in the visible, and water in the NIR. The dependence of the specific RI increment α of hemoglobin solution on the wavelength is in a good agreement with the literature data given by Friebel et al. for whole blood using an integrating sphere spectrometer technique and by Jung et al. for an Hb solution in intact individual RBC cytoplasm.[43,55]

As the experimental data for the real part of RI of hemoglobin solutions differ for measurements done by alternative techniques (see Table 4), it is important for researchers to use a specific tool, such as the Kramers–Kronig relations, to analyze experimental results for discrete wavelengths and to derive the RI real part theoretically from the measurements of its imaginary part.[4,24,49,50,53] In addition to providing quantification of the real part of the RI of hemoglobin at selected wavelengths, where no direct measurements are available, they are independent of hemoglobin concentration and thus can augment the model functions for the RI found by alternative methods.[4] Such analysis was done early in Ref. 4 for the measurements of the real part of the RI of hemoglobin solutions at eight discrete wavelengths from 400 to 700 nm, and we received encouraging results. In this work, measurements were done in a wider wavelength range from 480 to 1550 nm at 11 discrete wavelengths, which will allow us to make a more precise Kramers–Kronig analysis, results of which we are planning to publish in the near future.

5 Conclusion

The RI of hemoglobin solutions has been measured for visible and NIR ranges using a commercially available multiwavelength Atago refractometer. Data were approximated by the Sellmeier formula with a high accuracy in a whole wavelength range. The absolute value of the initial index of refraction n_0 and the specific refraction increment dn/dC on hemoglobin concentration C for room temperature at 23°C were derived from these measurements for each wavelength from 480 to 1550 nm. The data obtained are in good agreement with available data in the literature and supplementary to already measured values as done for new wavelengths, which allowed for evaluation of the specific refraction increment dn/dC in a wide spectral range.

Disclosures

The authors have no relevant financial interests in this article and no potential conflicts of interest to disclose.

Acknowledgments

The authors appreciate support from the Tomsk State University Competitiveness Improvement Programme, from the 5 top 100 Russian Academic Excellence Project at the Immanuel Kant Baltic Federal University (ENL), grants of the RFBR 17-02-00358 and the MES RF 17.1223.2017/AP (VVT).

References

1. J. J. J. Dirckx, L. C. Kuypers, and W. F. Decraemer, "Refractive index of tissue measured with confocalmicroscopy," *J. Biomed. Opt.* **10**(4), 044014 (2005).
2. T. L. Troy, D. L. Page, and E. M. Sevick-Muraca, "Optical properties of normal and diseased breast tissues: prognosis for optical mammography," *J. Biomed. Opt.* **1**(3), 342–355 (1996).
3. A. N. Bashkatov, E. A. Genina, and V. V. Tuchin, "Optical properties of skin, subcutaneous, and muscle tissues: a review," *J. Innovative Opt. Health Sci.* **4**(1), 9–38 (2011)
4. O. Sydoruk et al., "Refractive index of solutions of human hemoglobin from the near-infrared to the ultraviolet range: Kramers-Kronig analysis," *J. Biomed. Opt.* **17**(11), 115002 (2012).
5. L. V. Wang and H. I. Hu, *Biomedical Optics: Principles and Imaging*, John Wiley and Sons, Hoboken, New Jersey (2007).
6. V. V. Tuchin, *Tissue Optics: Light Scattering Methods and Instruments for Medical Diagnostics*, 3rd ed., PM 254, p. 988, SPIE Press, Bellingham, Washington (2015).
7. C. Meinke, M. Friebel, and J. Helfmann, "Optical properties of flowing blood cells," in *Advanced Optical Flow Cytometry: Methods and Disease Diagnoses*, V. V. Tuchin, Ed., pp. 95–132, Wiley-VCH Verlag GmbH & Co. KGaA, Weinheim (2011).
8. M. Meinke et al., "Optical properties of platelets and blood plasma and their influence on the optical behavior of whole blood in the visible to near infrared wavelength range," *J. Biomed. Opt.* **12**, 014024 (2007).
9. O. S. Zhernovaya, V. V. Tuchin, and I. V. Meglinski, "Monitoring of blood proteins glycation by refractive index and spectral measurements," *Laser Phys. Lett.* **5**(6), 460–464 (2008).

10. P. Giannios et al., "Complex refractive index of normal and malignant human colorectal tissue in the visible and near-infrared," *J. Biophotonics* **10**(2), 303–310 (2017).
11. S. Carvalho et al., "Wavelength dependence of the refractive index of human colorectal tissues: comparison between healthy mucosa and cancer," *J. Biomed. Photonics Eng.* **2**(4), 040307 (2016).
12. G. Popescu, *Quantitative Phase Imaging of Cells and Tissues*, McGraw-Hill, New York (2011).
13. H. Majeed et al., "Quantitative phase imaging for medical diagnosis," *J. Biophotonics* **10**(2), 177–205 (2017).
14. M. Shan, M. E. Kandel, and G. Popescu, "Refractive index variance of cells and tissues measured by quantitative phase imaging," *Opt. Express* **25** (2), 1573–1581 (2017).
15. M. E. Kandel et al., "Label-free tissue scanner for colorectal cancer screening," *J. Biomed. Opt.* **22**(6), 066016 (2017).
16. Z. Wang et al., "Tissue refractive index as marker of disease," *J. Biomed. Opt.* **16**(11), 116017 (2011).
17. T. H. Nguyen et al., "Automatic Gleason grading of prostate cancer using quantitative phase imaging and machine learning," *J. Biomed. Opt.* **22**, 036015 (2017).
18. H. Majeed et al., "Quantifying collagen fiber orientation in breast cancer using quantitative phase imaging," *J. Biomed. Opt.* **22**, 046004 (2017).
19. M. Lee et al., "Label-free optical quantification of structural alterations in Alzheimer's disease," *Sci. Rep.* **6**, 31034 (2016).
20. A. Greenbaum et al., "Wide-field computational imaging of pathology slides using lens-free on-chip microscopy," *Sci. Transl. Med.* **6**, 267ra175 (2014).
21. M. V. Volkenshtein, *Molecular Optics*, p. 96, Gosteskhizdat, Moscow (1951).
22. G. M. Hale and M. R. Querry, "Optical constants of water in the 200-nm to 200-μm wavelength region," *Appl. Opt.* **12**(3), 555–563 (1973).
23. D. Segelstein, "The complex refractive index of water," MS Thesis, Department of Physics, University of Missouri, Kansas City (1981).
24. L. X. Cundin and W. P. Roach, "Kramers-Kronig analysis of biological skin," arXiv:1010.3752v1 (2010).
25. K. Lee et al., "Measurements of complex refractive indices of photoactive yellow protein," arXiv:1507.00412 (2015).
26. Z. Deng et al., "Determination of continuous complex refractive index dispersion of biotissue based on internal reflection," *J. Biomed. Opt.* **21**(1), 015003 (2016).
27. F. P. Bolin et al., "Refractive index of some mammalian tissues using a fiber optic cladding method," *Appl. Opt.* **28**(12), 2297–2303 (1989).
28. M. Daimon and A. Masumura, "Measurement of the refractive index of distilled water from the near-infrared region to the ultraviolet region," *Appl. Opt.* **46**(18), 3811–3820 (2007).
29. D. K. Sardar and L. B. Levy, "Optical properties of whole blood," *Lasers Med. Sci.* **13**(2), 106–111 (1998).
30. G. J. Tearney et al., "Determination of the refractive index of highly scattering human tissue by optical coherence tomography," *Opt. Lett.* **20**, 2258–2260 (1995).
31. A. Knüttel, S. Bonev, and W. Knaak, "New method for evaluation of in vivo scattering and refractive index properties obtained with optical coherence tomography," *J. Biomed. Opt.* **9**(2), 265–273 (2004).
32. H.-C. Cheng and Y.-C. Liu, "Simultaneous measurement of group refractive index and thickness of optical samples using optical coherence tomography," *Appl. Opt.* **49**, 790–797 (2010).
33. I. Y. Yanina, N. A. Trunina, and V. V. Tuchin, "Photoinduced cell morphology alterations quantified within adipose tissues by spectral optical coherence tomography," *J. Biomed. Opt.* **18**(11), 111407 (2013).
34. F. E. Robles, S. Chowdhury, and A. Wax, "Assessing hemoglobin concentration using spectroscopic optical coherence tomography for feasibility of tissue diagnostics," *Biomed. Opt. Express* **1**(1), 310–317 (2010).
35. J. H. Jung et al., "Hyperspectral optical diffraction tomography," *Opt. Express* **24**(3), 2006–2012 (2016).
36. F. E. Robles et al., "Molecular imaging true-colour spectroscopic optical coherence tomography," *Nat. Photonics* **5**(12), 744–747 (2011).
37. Y. L. Jin et al., "Refractive index measurement for biomaterial samples by total internal reflection," *Phys. Med. Biol.* **51**(20), N371–N379 (2006).
38. A. García-Valenzuela and H. Contreras-Tello, "Optical model enabling the use of Abbe-type refractometers on turbid suspensions," *Opt. Lett.* **38**(5), 775–777 (2013).
39. H. Contreras-Tello and A. García-Valenzuela, "Refractive index measurement of turbid media by transmission of backscattered light near the critical angle," *Appl. Opt.* **53**(21), 4768–4778 (2014).
40. N. Lue and G. Popescu, "Live cell refractometry using microfluidic devices," *Opt. Lett.* **31**(18), 2759–2761 (2006).
41. Y. K. Park et al., "Spectroscopic phase microscopy for quantifying hemoglobin concentrations in intact red blood cells," *Opt. Lett.* **34**(23), 3668–3670 (2009).
42. F. E. Robles, L. L. Satterwhite, and A. Wax, "Non-linear phase dispersion spectroscopy," *Opt. Lett.* **36**(23), 4665–4667 (2011).
43. J.-H. Jung, J. Jang, and Y. K. Park, "Spectro-refractometry of individual microscopic objects using swept-source quantitative phase imaging," *Anal. Chem.* **85**(21), 10519–10525 (2013).
44. R. Barer, "Refractometry and interferometry of living cells," *J. Opt. Soc. Am.* **47**(6), 545–556 (1957).
45. D. J. Faber et al., "Oxygen saturation-dependent absorption and scattering of blood," *Phys. Rev. Lett.* **93**(2), 028102 (2004).
46. O. Zhernovaya et al., "The refractive index of human hemoglobin in the visible range," *Phys. Med. Biol.* **56**(13), 4013–4021 (2011).
47. J. Wang et al., "Measurement of the refractive index of hemoglobin solutions for a continuous spectral region," *Biomed. Opt. Express* **6**(7), 2536–2541 (2015).
48. M. Yahya and M. Z. Saghir, "Empirical modelling to predict the refractive index of human blood," *Phys. Med. Biol.* **61**, 1405–1415 (2016).
49. S. F. Shumilina, "Dispersion of real and imaginary part of the complex refractive index of hemoglobin in the range 450 to 820 nm," *Bullet. Beloruss. SSR Acad. Sci.* **1**, 79–84 (1984).
50. J. Gienger et al., "Determining the refractive index of human hemoglobin solutions by Kramers–Kronig relations with an improved absorption model," *Appl. Opt.* **55**(31), 8951–8961 (2016).
51. G. V. Maksimov et al., "Role of viscosity and permeability of the erythrocyte plasma membrane in changes in oxygen-binding properties of hemoglobin during diabetes mellitus," *Bull. Exp. Biol. Med.* **140**(5), 510–513 (2005).
52. J. Singh, *Optical Properties of Condensed Matter and Applications*, Wiley, Chichester (2006).
53. S. A. Prahl, "Optical absorption of hemoglobin," Oregon Medical Laser Center, http://omlc.ogi.edu/spectra/hemoglobin/index.html (3 March 2018).
54. M. Andersen and L. Painter, "Dispersion equation and polarizability of bovine serum albumin from measurements of refractive indices," *Biopolymers* **13**, 1261–1267 (1974).
55. M. Friebel and M. Meinke, "Model function to calculate the refractive index of native hemoglobin in the wavelength range of 250 to 1100 nm dependent on concentration," *Appl. Opt.* **45**(12), 2838–2842 (2006).
56. M. Friebel, "Determination of the complex refractive index of highly concentrated hemoglobin solutions using transmittance and reflectance measurements," *J. Biomed. Opt.* **10**(6), 064019 (2005).

Ekaterina N. Lazareva is an engineer at the Department of Optics and Biophotonics of Saratov State University. Her research interests are in optical properties of biological tissues, especially of blood (its components) and adipose tissue, refractometry and spectroscopy of tissues, and tissue optical clearing.

Valery V. Tuchin is a professor and head of optics and biophotonics at Saratov State University (National Research University of Russia) and several other universities. His research interests include tissue optics, laser medicine, tissue optical clearing, and nanobiophotonics. He is a fellow of SPIE and OSA, has been awarded Honored Science Worker of the Russia, Honored Professor of Saratov University, SPIE Educator Award, FiDiPro, Finland, Chime Bell Prize of Hubei Province, China, NanQiang Life Science Series Lectures Award of Xiamen University, China, and the Joseph W. Goodman Book Writing Award (OSA/SPIE).